FEM Analysis of a FGM Pre-Stressed Plate Strip With A Circular Hole Under Bending

Ulku Babuscu Yesil[1,*] and Mehmet Can Atasayanlar[1]

[1] 1,2-Yildiz Technical Uni., Faculty of Chemical and Metallurgical Eng., Dep. of Mathematical Engineering, Istanbul, Turkey
[*] Corresponding author. E-mail: ubabuscu@yildiz.edu.tr

Received: Apr. 20, 2020, Accepted: Jun. 16, 2020

A static analysis of a pre-stressed plate-strip made from functionally-graded material (FGM) containing a circular hole has been investigated under bending forces. The plate-strip is simply supported on two opposite ends and the pre-stresses are formed by the uniformly distributed forces which acts on these two ends before the main loading. The influences of pre-stresses in the plate-strip on the distributions of displacements and stresses around the hole caused by the additional bending forces acting on the upper face-plane of the FGM plate-strip are investigated. The Linearized Three-Dimensional Elasticity Theory and the generalized plane-strain conditions are assumed for the modelling of the theoretical investigations.
Young's modulus of the medium varies continuously in the horizontal and vertical directions according to power law distribution, but the Poisson's ratio and material density are assumed to be constant. The solution of the considered problem is obtained numerically with the help of the Finite Element Method (FEM). Numerical results of distributions of the displacements and stresses around the hole are presented and discussed for various problem parameters such as, material property, plate size, initial effect and position of the hole.

Keywords: Functionally graded material; Initial stress; Circular hole; Static analysis; FEM

http://dx.doi.org/10.6180/jase.202012_23(4).0007

1. Introduction

Functionally Graded Materials (FGM) is a new material concept wherein material properties vary continuously from one point to another in some specific directions, FGM is widely used in many engineering applications due to their high strength and thermal resistance, such as chemical engineering, electronic engineering, biology, aerospace, biomedicine etc.

FGM were first used in Japan on a spacecraft project in 1984. A concept of FGM was given in [1]. Since then, the interest of researchers on the mechanics of FGM has gradually increased, and in the last 20 years many numerical, experimental and theoretical studies have been conducted. Some plane elasticity problems and analytical solutions were given for plates made of FGM with and without cracks under different boundary conditions in [2]. Axisymmetric bending and stretching of functionally graded solid and annular circular plates was examined using the first-order shear deformation Mindlin plate theory in [3]. Graded finite elements were formulated using linear interpolation functions to model the behavior of inhomogeneous materials in [4]. Graded finite elements were presented using a generalized isoparametric formulation in [5]. The formulations of the series solutions of the FGM plates were derived in [6] and numerical solutions of theoretical formulations of this study were studied by FEM using MARC program in [7]. Multiple isoparametric finite element formulation was used to examine the influence of the material property inhomogeneity on the stress concentration factor due to a circular hole in functionally graded panels [8]. Elasticity solutions for the axisymmetric problem of a functionally graded annular plate under uniformly loading was investigated in [9].

A complex variable method was presented for calculating stress distribution around a circular hole in a FGM plate in [10]. The least square boundary collocation technique combined with complex variable method was used for calculating two dimensional stress distribution of a fi-

nite FGM plate with a circular hole under arbitrary constant loads [11]. A comprehensive review of FGM has been made in [12]. Geometrically nonlinear analysis of planar beam and frame structures made of FGM by using finite element method was studied in [13]. The modelling of the FG beam resting in/on an accurately conceived soil medium continuum was investigated on both dynamic and static loading in [14]. Higher order shear deformation theory for FGM plates was proposed in [15]. An alternative solution procedure by using Gateaux differential method for analysis of shear deformable FGM beams with mixed formulation was studied in [16]. The static behavior of FGM beams was investigated using 3D Saint-Venant's theory in [17]. Static analysis of a square functionally graded sandwich plate was investigated by using the four variable plate theory in [18].

However, there are no research studies on preliminary effects, such as pre-stresses in the structural element for FGM. The aim of the present investigation is to determine the influence of initial stresses on static analysis of FGM plates with a hole under bending. The distributions of stresses and displacements caused by the action of additional uniform loading may significantly affected with initial stresses. The superposition principle can not be applicable to these problems. Thus, mathematical modeling of the problem is carried out within the framework of the Linearized Three Dimensional Theory of Elasticity that is obtained by linearizing the three dimensional nonlinear theory of elasticity. FEM is employed to solve the corresponding boundary-value problem. The numerical results on the effect of the pre-stresses and varying material properties of FGM on the distributions of displacements and stresses caused by the additional uniform loading are presented.

2. Mathematical Backgrounds

The geometry and loading of the plate-strip are given in Fig. 1. The plate-strip is simple supported at two edges and the pre-stresses in its structure being formed by the uniformly distributed normal force acting on these two edges and having a unit density q (Fig. 1a). Beside, the additional uniformly distributed normal forces with a unit density p act on the upper face-plane of the plate (Fig. 1b). Since the plate-strip discussed is functional, the material properties depend on the coordinates. As mentioned in most studies on the FGM, the effect of Poisson's ratio which is a function of coordinates on the distributions of stresses and displacements can be omitted. Poisson's ratio is assumed to be constant.

Two different problems will be discussed in which the Young Module changes with respect to the horizontal direction (Ox_1 axis) and vertical direction (Ox_2 axis) according to power-law distribution, respectively. Two problems are solved according to the variation of Young Module; in the first (second) problem Young Module varies according to Ox_1 (Ox_2) axis. The following functional forms are used for the nodal values of Young's modulus;

$$\begin{aligned} &\textbf{Problem1: } E(x_1,x_2) = E(x_1) = E_0\,(ax_1+b)^n \ (\mathbf{x_1}-\mathbf{FGM}) \\ &\textbf{Problem2: } E(x_1,x_2) = E(x_2) = E_0\,(cx_2+d)^n \ (\mathbf{x_2}-\mathbf{FGM}), \\ &E_0, a, b, c, d, n \in R \end{aligned} \tag{1}$$

where E_0 (E_1) is the Young's modulus at $x_i = 0$ ($x_1 = \ell/2$ or $x_2 = h$) and n is the exponent of the power law material variation. There are two cases occur; if $E_0 < E_1$ then FGM progressively stiffens else if $E_0 > E_1$ then FGM progressively softens along the considered direction.

These problems are solved for a half of the domain, because of the symmetry of the geometry and loading with respect to the planes $x_1/\ell = 1/2$. The material property gradient around the circular hole for the half of the solution domain is shown for the Problem 1 (Problem 2) in Fig. 2a (Fig. 2b).

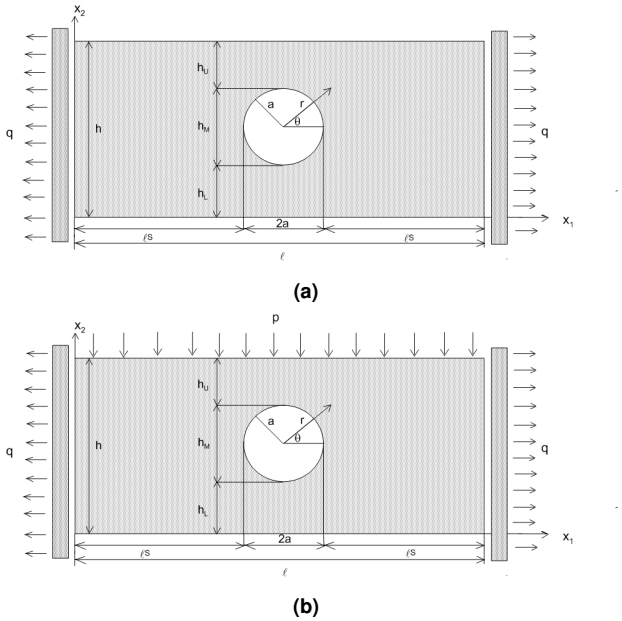

Fig. 1. (a) Loading of the rectangular plate-strip including circular hole in the (a) initial and (b) perturbed stage.

The mathematical model of the problem is made in the framework of the Linearized Three Dimensional Elasticity Theory under plane strain-state. For the solution procedure, considered problems are examined in two stages: the initial and perturbed stages. In the initial stage the consid-

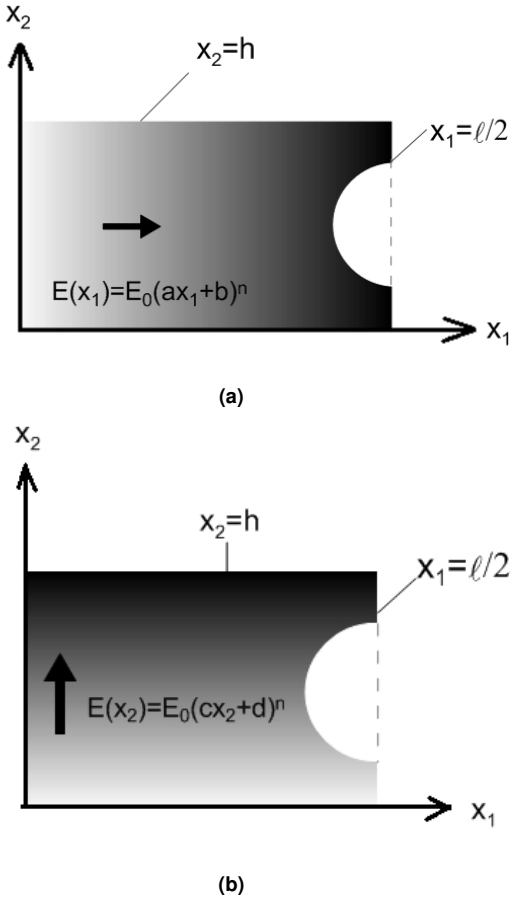

Fig. 2. Half FGM plate-strip with material properties varying over (a) Ox_1 axis (Problem 1) and, (b) Ox_2 axis (Problem 2).

ered FGM plate-strip with a hole is subjected to uniformly distributed normal stretching forces of intensity q acting on two opposite edges. After solution to considered problem in the first stages, stresses called as pre-stresses are determined in the plate-strip. In the perturbed stage assumed that this pre-stressed FGM plate-strip with a hole is subjected to additional uniformly distributed normal forces intensity of which is p (« q) on its upper face plane. For simplicity of notation, superscript 0 (1) denotes the quantities referring to the initial (perturbed) stage.

Solution domain of boundary value problem (BVP) is;

$$\begin{gathered}\Omega' = \Omega - \Omega_{\mathbf{h}} \\ \Omega = \{0 \le x_1 \le \ell; 0 \le x_2 \le h\} \\ \Omega_h = \\ \left\{(x_1, x_2) \mid (x_1 - (\ell_s + a))^2 + (x_2 - (h_L + a))^2 \le a^2\right\}\end{gathered} \tag{2}$$

The solution domain is discretized a finite number of sub-domains (FEs) and the solution in each sub-domain is considered as a polynomial function. For the FGM plate-strip, the displacement functions for each finite element can be written as;

$$\left\{ \begin{array}{c} u_1^{(e)} \\ u_2^{(e)} \end{array} \right\} = \sum_{i=1}^{n} N_i \left\{ \begin{array}{c} u_{1i}^{(e)} \\ u_{2i}^{(e)} \end{array} \right\}, e = 1, 2, \ldots, M \tag{3}$$

In (3), N_i is the shape function, u_{ki} is the nodal displacement corresponding to node i in the k direction, n is total number of nodal points in the element, M is total number of finite elements in the solution domain.

As usual, strain functions are derived from displacements by differentiation as

$$\varepsilon^{(e)} = \mathbf{B}^{(e)} \mathbf{u}^{(e)} \tag{4}$$

where $u^{(e)}$ is the nodal displacement vector and $B^{(e)}$ is the displacement-strain matrix of shape function derivatives.

Thus stress-strain relations can be given by

$$\sigma^{(e)} = \mathbf{D}^{(e)}(x_1, x_2)\, \varepsilon^{(e)} \tag{5}$$

where $D^{(e)}(x_1, x_2)$ is the constitutive matrix, which is a function of position of points. So, $D_{ij}^{(e)} = D_{ij}^{(e)}(x_1)$ (Problem 1) or $D_{ij}^{(e)} = D_{ij}^{(e)}(x_2)$ (Problem 2). The elements of this matrix can be given for the constant Poisson ratio;

$$\begin{gathered} D_{11} = D_{22} = \frac{(1-v)E(x_i)}{(1+u)(1-2v)}, \\ D_{12} = D_{21} = \frac{vE(x_i)}{(1+v)(1-2v)}, D_{66} = \frac{E(x_i)}{2(1+v)} \end{gathered} \tag{6}$$

where i=1 (2) for Problem 1 (2). The pre-stresses in the structure of the FGM plate-strip are determined with the help of classical linear elasticity theory in the initial stage. Equations and relations provided in the solution domain of the initial stage;

$$\begin{gathered} \frac{\partial \sigma_{ij}^{(0)}}{\partial x_j} = 0 \\ \sigma^{(0)} = D(x_i)\, \varepsilon^{(0)}, \sigma^{(0)} = \left[\sigma_{11}^{(0)}, \sigma_{22}^{(0)}, \tau_{12}^{(0)}\right], \varepsilon^{(0)} = \\ \left[\varepsilon_{11}^{(0)}, \varepsilon_{22}^{(0)}, \gamma_{12}^{(0)}\right] \\ \varepsilon_{ij}^{(0)} = \frac{1}{2}\left(\frac{\partial u_i^{(0)}}{\partial x_j} + \frac{\partial u_j^{(0)}}{\partial x_i}\right), i, j = 1, 2 \\ u_2\big|_{\substack{x_1=0;\ell \\ x_2 \epsilon [0,h]}} = 0, \sigma_{11}^{(0)}\Big|_{\substack{x_1=0;\ell \\ x_2 \epsilon [0,h]}} = 0, \sigma_{12}^{(0)}\Big|_{\substack{x_1=0;\ell \\ x_2 \epsilon [0,h]}} = 0, \sigma_{ij}^{(0)}\Big|_{\substack{x_2=0;h \\ x_1 \in [0,\ell]}} = 0, \\ \sigma_{ij}^{(0)} n_j\Big|_S = 0, \quad i, j = 1, 2 \\ S = \left\{(x_1, x_2) \mid (x_1 - (\ell_s + a))^2 + (x_2 - (h_L + a))^2 = a^2\right\} \end{gathered} \tag{7}$$

In (7), S is the rim of circular hole, n_j is the component of unit normal vector on the rim of circular hole. The

mathematical model of the BVP in the perturbed stage is given below [19]:

$$\begin{aligned}
&\frac{\partial}{\partial x_j}\left(\sigma_{ji}^{(1)}+\sigma_{in}^{(0)}\frac{\partial u_i^{(1)}}{\partial x_n}\right)=0\\
&\boldsymbol{\sigma}^{(1)}=\mathbf{D}\left(x_i\right)\boldsymbol{\varepsilon}^{(1)}\\
&\varepsilon_{ij}^{(1)}=\frac{1}{2}\left(\frac{\partial u_i^{(1)}}{\partial x_j}+\frac{\partial u_j^{(1)}}{\partial x_i}\right),i,j=1,2\\
&u_2^{(1)}\Big|_{\substack{x_1=0;\ell\\ x_2\epsilon[0,h]}}=0,\ \left(\sigma_{j1}^{(1)}+\sigma_{1n}^{(0)}\frac{\partial u_1^{(1)}}{\partial x_n}\right)n_j\Big|_{\substack{x_1=0;\ell\\ x_2\epsilon[0,h]}}=0\\
&\left(\sigma_{jk}^{(1)}+\sigma_{kn}^{(0)}\frac{\partial u_k^{(1)}}{\partial x_n}\right)n_j\Big|_{\substack{x_2=h\\ x_1\epsilon[0,\ell]}}\\
&=p\delta_2^k,\ \left(\sigma_{ji}^{(1)}+\sigma_{in}^{(0)}\frac{\partial u_i^{(1)}}{\partial x_n}\right)n_j\Big|_{\substack{x_2=0\\ x_1\epsilon[0,\ell]}}=0\\
&\left(\sigma_{ji}^{(1)}+\sigma_{in}^{(0)}\frac{\partial u_i^{(1)}}{\partial x_n}\right)n_j\Big|_S=0,\quad i;j;k=1,2
\end{aligned}\tag{8}$$

Note that if the pre-stresses in the structure is omitted in the perturbed stage (8) i.e. $\sigma_{in}^{(0)}=0$, these problem coincide with the corresponding problem modeled in the framework of the clasical theory of elasticity.

3. FEM Modeling of the problem

For the FEM modeling of the BVP (7) the functional

$$\begin{aligned}
&\Pi^{(0)}=\tfrac{1}{2}\iint_{\Omega'}\sigma_{ij}^{(0)}\varepsilon_{ij}^{(0)}dx_1dx_2\\
&-\int_0^h qu_1^{(0)}\Big|_{x_1=0}dx_2+\int_0^h qu_1^{(0)}\Big|_{x_1=\ell}dx_2,i;j=1,2
\end{aligned}\tag{9}$$

and for the FEM modelling of the BVP (8) the functional

$$\Pi^{(1)}=\frac{1}{2}\iint_{\Omega'}\left(T_{ij}\frac{\partial u_j}{\partial x_i}\right)dx_1dx_2-\int_0^{\ell}pu_2^{(1)}\Big|_{x_2=h}dx_1 \tag{10}$$

where

$$T_{ij}\left(x_k\right)=\sigma_{ij}^{(1)}+\sigma_{in}^{(0)}\frac{\partial u_i^{(1)}}{\partial x_n},\quad i;j;k=1,2 \tag{11}$$

are used [20]. In (9)-(11) components of σ_{ij}, T_{ij} are functions of position of points. The principle of virtual work and Ritz technique yield the following finite element stiffness equation;

for the initial stage;

$$\mathbf{K}^{(0)}\mathbf{u}^{(0)}=F^{(0)} \tag{12}$$

and for the perturbed stage

$$\mathbf{K}^{(1)}\mathbf{u}^{(1)}=F^{(1)} \tag{13}$$

where $F^{(0)}, F^{(1)}$ are the load vectors, $K^{(0)}, K^{(1)}$ are the Stiffness matrices, $u^{(0)}, u^{(1)}$ are the nodal displacements vectors and the element stiffness matrix $\mathbf{K}^{(0)e}$ or $\mathbf{K}^{(1)e}$ is

$$\mathbf{K}^{(s)e}=\int_{\Omega_e}\left(B^{(s)e}\right)^T D^{(s)e}B^{(s)e}d\Omega_e \tag{14}$$

where Ω_e $\left(\Omega=\bigcup_{e=1}^{M}\Omega_e\right)$ is the domain of e^{th} finite element and T indicates transpose, $s=0$ $(s=1)$ for the first (second) stage, $D_{ij}^{(e)}=D_{ij}^{(e)}\left(x_1\right)$ (Problem 1) or $D_{ij}^{(e)}=D_{ij}^{(e)}\left(x_2\right)$ (Problem 2). Nodal displacements are obtained by solving the equations 12 and 13 , however Eq. 13 includes the values of stresses from the initial stage. So, the stress distributions for the initial stage should be known before finding the solution of Eq. 13. In each finite element Gauss quadrature method with 10 sample points is used to obtain the numerical values of definite integrals.

The solution domain Ω' is divided into 8 curvilinear triangular FEs with 6 nodes and Nine-noded quadrilateral (Q9) elements are used for the domain not covered by the triangular FEs. The formulation of the standard shape functions are;

For corner nodes;

$$N_i=\frac{1}{4}\xi\eta\left(\xi+\xi_i\right)\left(\eta+\eta_i\right) \tag{15}$$

For mid-side nodes;

$$\begin{aligned}
&\xi_i=0\Rightarrow N_i=\tfrac{1}{2}\eta\left(1-\xi^2\right)\left(\eta+\eta_i\right)\\
&\eta_i=0\Rightarrow N_i=\tfrac{1}{2}\xi\left(\xi+\xi_i\right)\left(1-\eta^2\right)
\end{aligned}\tag{16}$$

For center node;

$$N_i=\left(1-\xi^2\right)\left(1-\eta^2\right) \tag{17}$$

where (ξ,η) indicate normalized coordinates in the interval [-1,1] and (ξ_i,η_i) indicate the local coordinates of node i.

The formulation of the shape functions for the triangular FEs are;

$$N_i\left(x_1,x_2\right)=a_i+b_ix_1+c_ix_2+d_ix_1^2+e_ix_1x_2+f_ix_2^2 \tag{18}$$

The unknown coefficients of the Eq. 18 for each node can be found with

$$N_i\left(x_{1j},x_{2j}\right)=\delta_{ij} \tag{19}$$

where δ_{ij} is the Kronecker symbol and $\left(x_{1j},x_{2j}\right)$ are the coordinates of j -th node in the Ox_1x_2 coordinate. The same finite element discretization is used in finite element solution of BVPs of both stages

4. Result discussions

A half model is used because of the symmetry of the problem about the x_1 axis. Solution domain is divided into 80 and 12 rectangular elements along the Ox_1 and Ox_2 axes, respectively. In the FEM modeling, a total of 956 rectangular elements with 9 nodes, 8 curved edges triangular finite elements surrounded the circular hole with 6 nodes, totally 4027 nodes and 8004 NDOFs are employed. FE discretization of the solution domain is selected among the finite element meshes in which the numerical results found for many finite elements' meshes are best approached to the corresponding numerical results in the literature. It should be noted that the graphs of the displacements and stresses obtained for the Problem 1 (Problem 2) are given according to the axis $Ox_1(Ox_2)$. In the present study, Poisson's ratio is assumed to be constant and set to be $v = 0.3$.

The main aim of the present numerical investigations is to determine how the pre-stresses effect the stresses and displacements around the hole in the FGM plate-strip under bending. Before considering the main numerical results, for testing of the used calculation algorithm and programs which are composed by the authors and realized in FORTRAN 77. First it is considered the numerical results obtained for the case where the material of the plate-strip is isotropic and contains a circular hole in the initial stage.

In the case of homogeneous material of the infinite plate, the distribution of the stress $(\sigma_{\theta\theta})$ is given [21]

$$\sigma_{\theta\theta} = q(1 - 2\cos 2\theta) \tag{20}$$

In this study if the plate size is much bigger than the hole-diameter, our numerical results should close to the results (20) given for the infinite plate. So, in the initial stage (Fig. 1a), by decreasing a/ℓ or increasing ℓ_S/a, stress distribution for an infinite plane containing a circular hole must be obtained given in [21, 22].

Table 1 show the results determined by employing the present algorithm overlap with the corresponding ones obtained in the paper [21, 22].

Focusing second on Fig. 3 Fig. 3a (b) show some sample results for the stress distribution of $\sigma_{11}^{(1)}/p$ in the unholed medium for Problem (2) obtained from [23] ([2]) for some values of the material nonhomogeneity parameter E_1/E_0. These numerical results obtained for graded plate-strip without a hole under bending for both problems. In problem 1 (2); material properties varying over Ox_1 (Ox_2) axes. Notice that the graded solution and the exact solution is identical.

Since dimensionless quantities are used in the numerical calculation, the ratio of E_1/E_0 represent the largest Young modulus in the plate-strip. For instance, $E_1/E_0 = 1$ corresponds to the case where the plate-strip material is homogeneous.

Table 1. The stress concentration of $\sigma_{\theta\theta}^{(0)}$ / q at the given values of θ around the hole for the isotropic plate-strip with a circular hole

ℓ_S/a	a/ℓ	θ		
		$3\pi/4$	$\pi/2$	π
17.41	0.0140	1.0388	3.2156	-0.9513
18.75	0.0130	1.0319	3.1751	-0.9382
19.50	0.0125	1.0284	3.1538	-0.9317
20.31	0.0120	1.0247	3.1316	-0.9252
22.15	0.0110	1.0173	3.0339	-0.9122
24.37	0.0100	1.0099	3.0303	-0.8987
25.39	0.0096	1.0071	3.0068	-0.8931
∞	–	1.0	3.0	-1

In Fig. 3a (3b), if the plate-strip has the FGM property in the direction of Ox_1(Problem 1) $(Ox_2$(Problem 2)), graphics approach to the graphic given in the homogeneous plate as E_1/E_0 decreases, and for the case where $E_1/E_0 = 1$ the results overlap with the exact analytical solution given in [23]([2]). These results also verify the correctness of the programs and algorithm made by the authors.

Fig. 4 (Fig. 5) compare the effect of initial compressive force (i.e. $q/E_O < 0$) versus initial stretching force on the normalized tangential stress (normalized radial stress) distribution of finite FGM plate in the case where $h/\ell = 0.15, h_u/a = 5, E_1/E_0 = 5, n = 2$ and Young's Modulus is given as Eq. 1. The effect of initial compressive force (i.e. $q/E_O < 0$) is shown as dashed lines in the figures. It is found that the stress distribution around the hole is affected from the initial compressive force much more than the corresponding values of the initial stretching force (i.e. $q/E_0 > 0$). The absolute values of stresses of $\sigma_{\theta\theta}^{(1)}/p$ and $\sigma_{rr}^{(1)}/p$ increase (decrease) with the absolute values of q/E_0 under compression (initial tension).

Fig. 6 (Fig. 7) compare the effect of initial compressive force (i.e. $q/E_0 < 0$) versus initial stretching force on the distribution of the normalized radial (normalized tangential) displacement of finite FGM plate with hole in the case where $h/\ell = 0.15, h_u/a = 5$ $E_1/E_0 = 5, n = 2$ and Young's Modulus is given as eq. 1. The effect of initial compressive force (i.e. $q/E_0 < 0$) is shown as dashed lines in the figures. It is found that the both displacement distributions around the hole is affected from the initial compressive force much more than the corresponding values of the initial stretching

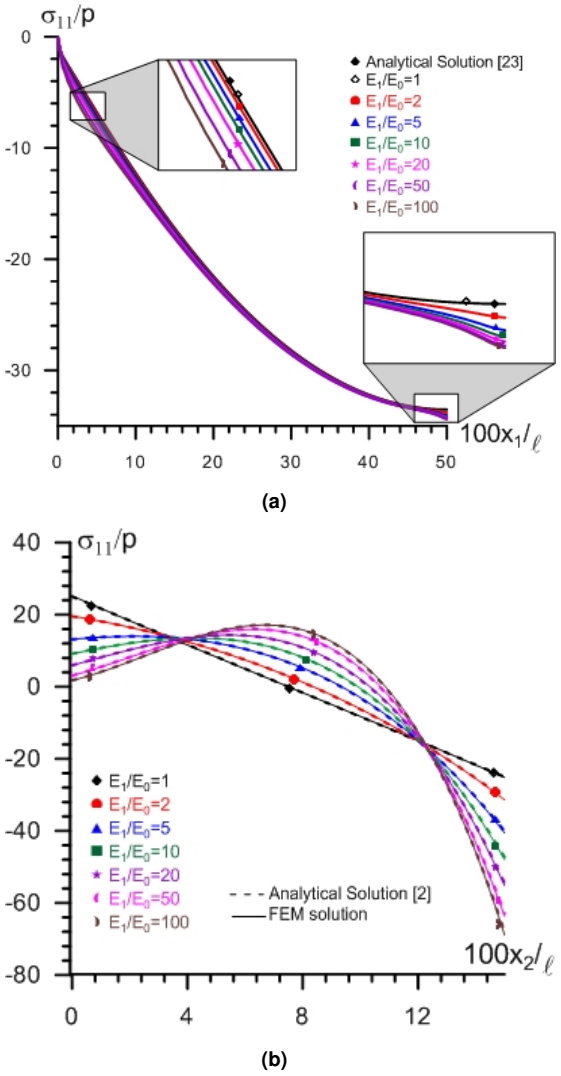

Fig. 3. Comparison of FE results and exact equations of stress distribution of $\sigma_{11}^{(1)}/p$ under bending for $q/E_0 = 0$ for (a) Problem 1 along the Ox_1, axis in $x_2 = h$ plane (b) Problem 2 along the Ox_2 axis in $x_1 = \ell/4$ plane.

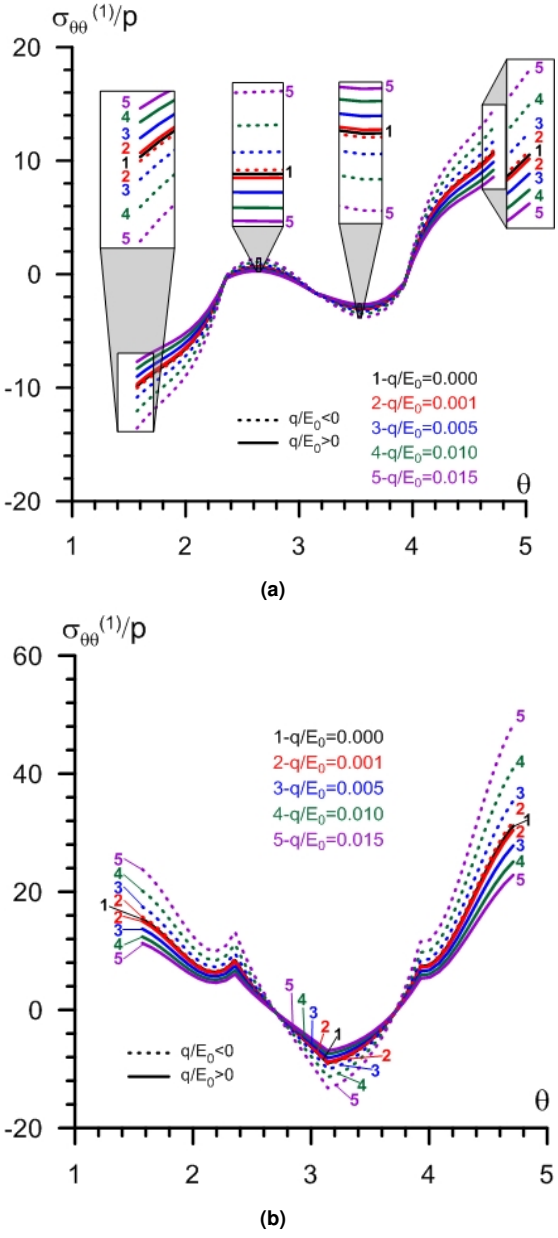

Fig. 4. The normalized tangential stress $\sigma_{\theta\theta}^{(1)}/p$ on the rim of circular hole around $\theta \in [-\pi/2, +\pi/2]$ for the different pre-stresses under $E_1/E_0 = 5, h_u/a = 5$ and h / $\ell = 0.15, n = 2$ for (a)Problem1(b)*Problem*2.

force. The absolute values of the displacements $u_r^{(1)}/\ell$ and $u_\theta^{(1)}/\ell$ increase (decrease) with the absolute values of q/E_0 under compression (initial tension). The variation of pre-stresses does not change the position of the displacements' maximum. The absolute maximum values of $u_r^{(1)}/\ell$ occur at the poles $\theta = \pm\pi/2$ and the absolute maximum values of $u_\theta^{(1)}/\ell$ occur at the pole $\theta = \pi$

The variation of normalized tangential (radial) stress around the circular hole is plotted in Fig. 8 (Fig. 9) for different size of the plate-strip (i.e., h/ℓ) for both the $q/E_0 = 0$ and $q/E_0 = 0.005$ where $h_u/a = 5, n = 2, E_1/E_0 = 5$. An increase in the values of h/ℓ, causes a decrease in the absolute values of stresses for both problems. The difference between the values obtained for $q/E_0 = 0$ and $q/E_0 = 0.005$ also decrease with h/ℓ.

The variation of normalized radial (tangential) displacement around the circular hole is plotted in Fig. 10 (Fig. 11) for different size of plate-strip (i.e., h/ℓ) for two cases of q/E_0 (i.e. $q/E_0 = 0; q/E_0 = 0.005$) where $h_u/a = 5, n = 2, E_1/E_0 = 5$. An increase in the value of h/ℓ cause a decrease in the absolute values of displacements for both

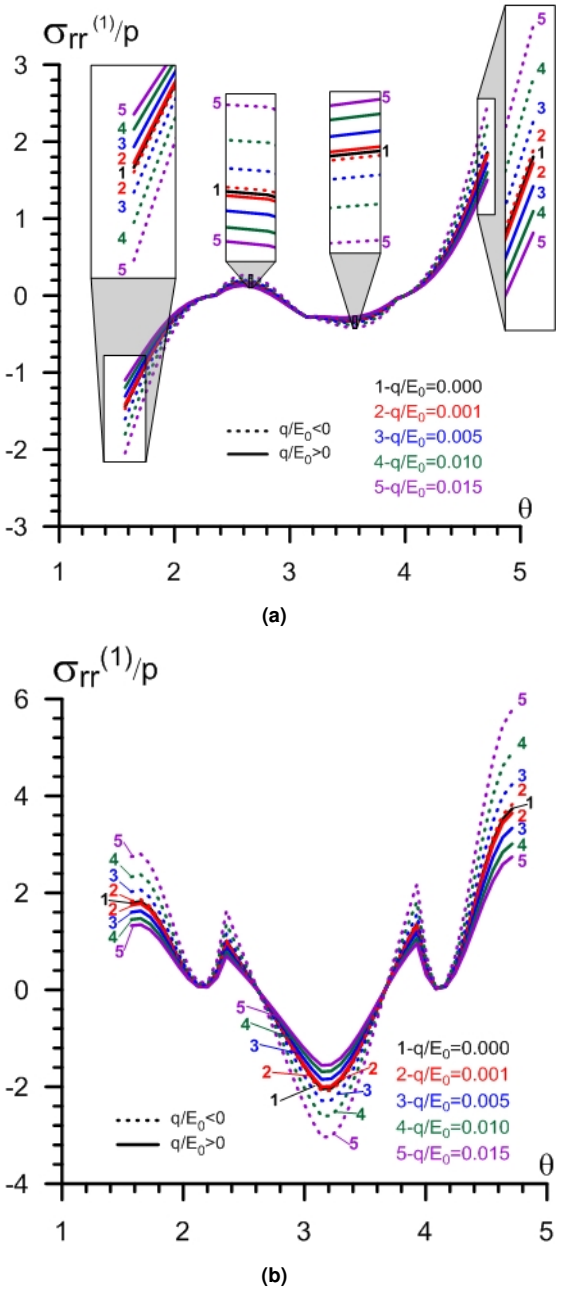

Fig. 5. The normalized radial stress $\sigma_{rr}^{(1)}/p$ on the rim of circular hole around $\theta \in [-\pi/2, +\pi/2]$ for the different pre-stresses under $E_1/E_0 = 5,\ h_u/a = 5$ and $h/\ell = 0.15,\ n = 2$ for (a) Problem 1 (b), Problem 2.

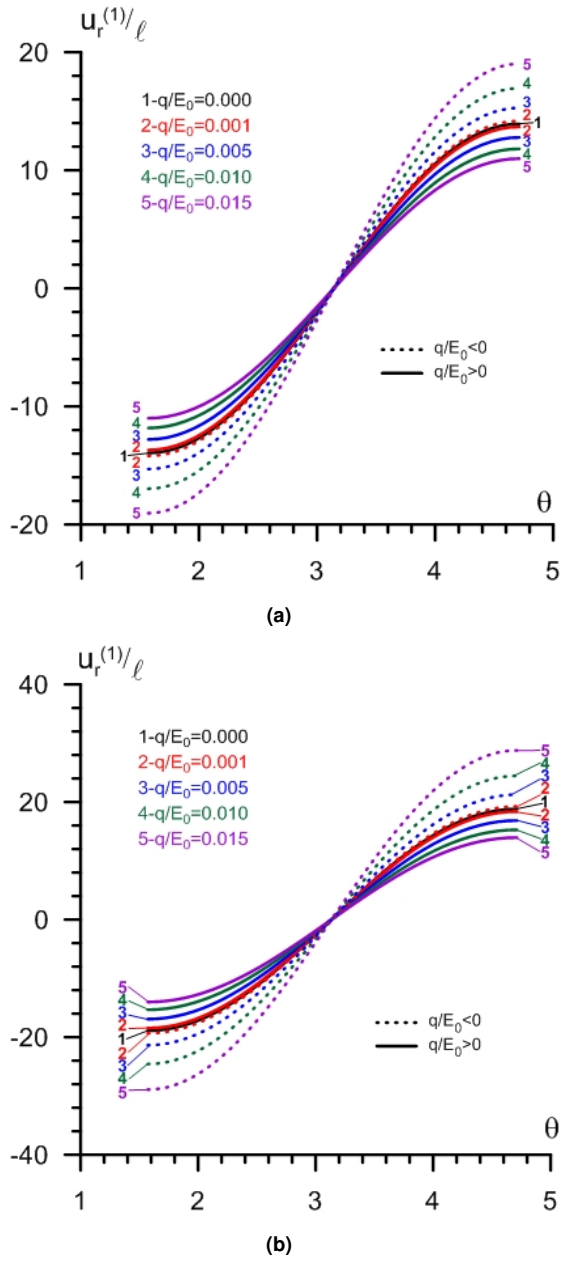

Fig. 6. The normalized radial displacement $u_r^{(1)}/\ell$ on the rim of circular hole around $\theta \in [-\pi/2, +\pi/2]$ for the different pre-stresses under $E_1/E_0 = 5,\ h_u/a = 5$ and $h/\ell = 0.15, n = 2$ for (a) Problem 1 (b) Problem 2.

problems. The difference between the values obtained for $q/E_0 = 0$ and $q/E_0 = 0.005$ also decrease with h/ℓ

Figs. 12, 13 and 14 plot the variation of normalized stresses $\sigma_{\theta\theta}^{(1)}/p$, $\sigma_{\mathrm{rr}}^{(1)}/\mathrm{p}$ and $\tau_{\mathrm{r}\theta}^{(1)}/\mathrm{p}$ respectively, for different location of hole for two cases of q/E_0 (i.e., q/E_0 = $_0$; q/E_0 = $_{0,005}$) where h/ℓ = 0.15, n = 2, $E_1/E_0 = 5$. The location of the hole is characterized by the parameter $h_u/$ a, which shows the distance between the upper surface of the circular hole and the upper face of the plate. It follows from the graphs that the absolute values of the stresses increase with decreasing the parameter $h_u/$ a for both cases of q/E_0.

The normalized tangential and radial displacements around the circular hole are plotted for two cases of q/E_0 where h/ℓ = 0.15, h_u/a = 5 and $E_1/E_0 = 5$ in Fig. 15 and Fig. 16 respectively, according to the changes of power-law

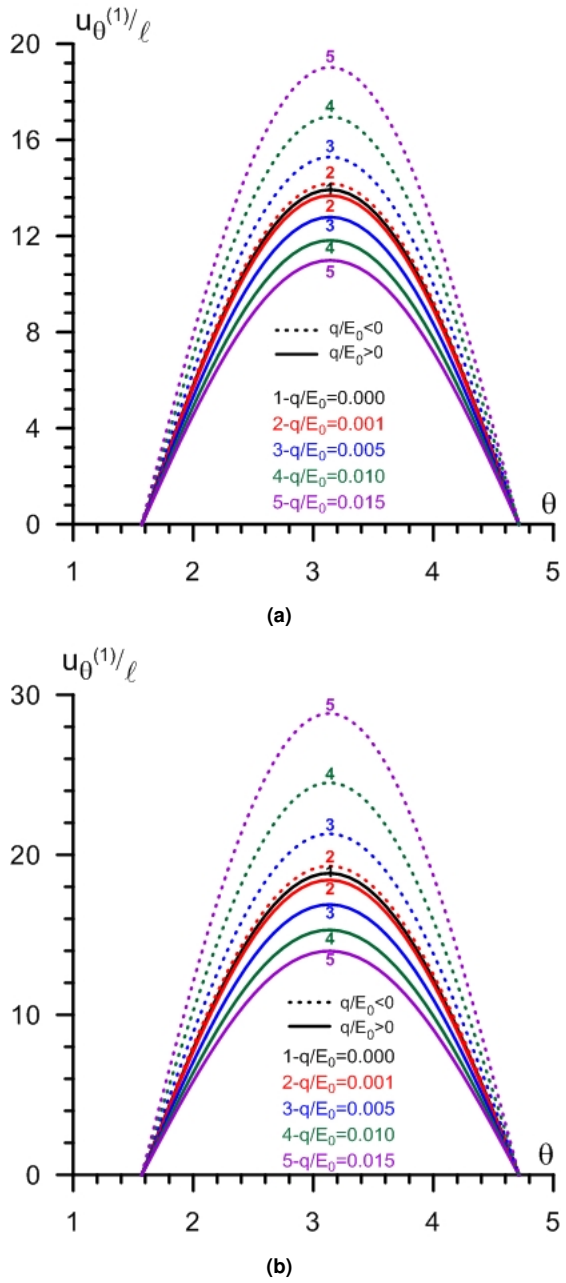

Fig. 7. The normalized tangential displacement $u_\theta^{(1)}/\ell$ on the rim of circular hole around $\theta \in [-\pi/2, +\pi/2]$ for the different pre-stresses under $E_1/E_0 = 5, h_u/a = 5$ and

$h/\ell = 0.15, n = 2$ for

(a) Problem 1 (b) Problem 2

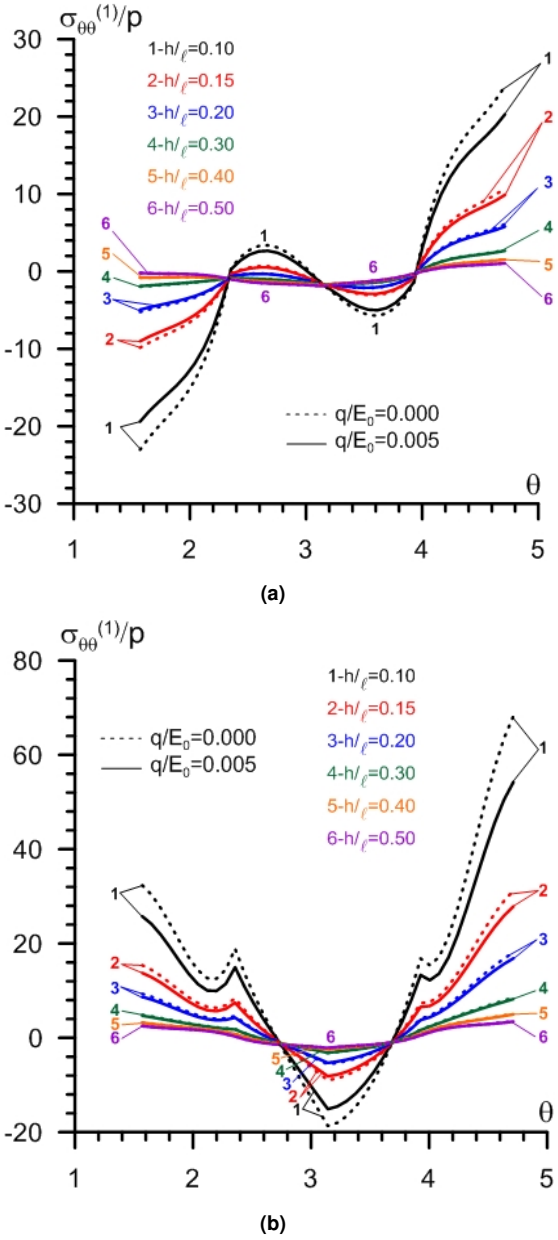

Fig. 8. The normalized tangential stress $\sigma_{\theta\theta}^{(1)}/p$ on the rim of circular hole around $\theta \in [-\pi/2, +\pi/2]$ for the different thickness of the plate-strip (i.e., h/ℓ) under $E_1/E_0 = 5, h_u/a = 5$ and $n = 2$ for two cases of q/E_0 for (a) Problem 1 (b) Problem 2

exponent value, i.e., n. All the displacements around the hole increase with the power-law exponent value (n). The presence of initial stress reduces the effect of **n**

The influence of Young's Modulus ratio (E_1/E_0) on the normalized radial and tangential displacement are investigated base on two n values, i.e., $n = 0.5$ and $n = 2$ in Fig. 17 and Fig. 18, respectively under $q/E_0 = 0.005$, h / $\ell = 0.15$, $h_u/a = 5$ for (a) Problem 1, (b) Problem 2. It can be seen that for a certain value of **n**, the displacement decreases with increasing Young's Modulus ratio. Also, the displacements increase with the power-law exponent value, while the displacements does not alter with the in-

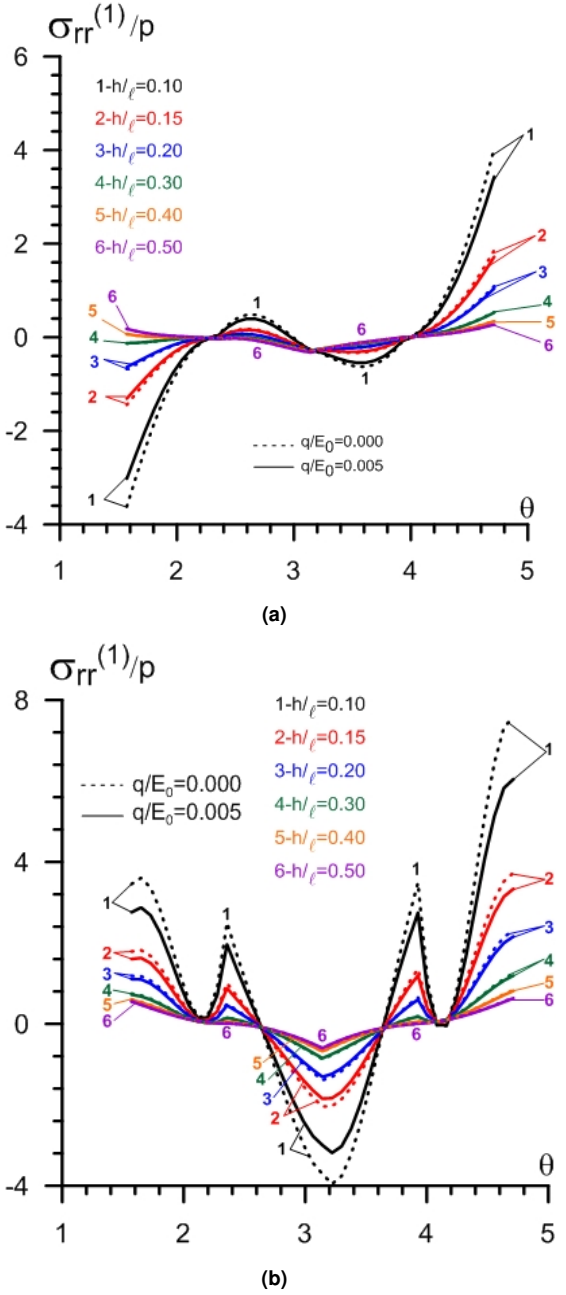

Fig. 9. The normalized radial stress $\sigma_{rr}^{(1)}/p$ on the rim of circular hole around $\theta \in [-\pi/2, +\pi/2]$ for the different thickness of the plate-strip (i.e., h/ℓ) under $E_1/E_0 = 5$, $h_u/a = 5$ and $n = 2$ for two cases of q/E_0 for (a) Problem 1, (b) Problem 2.

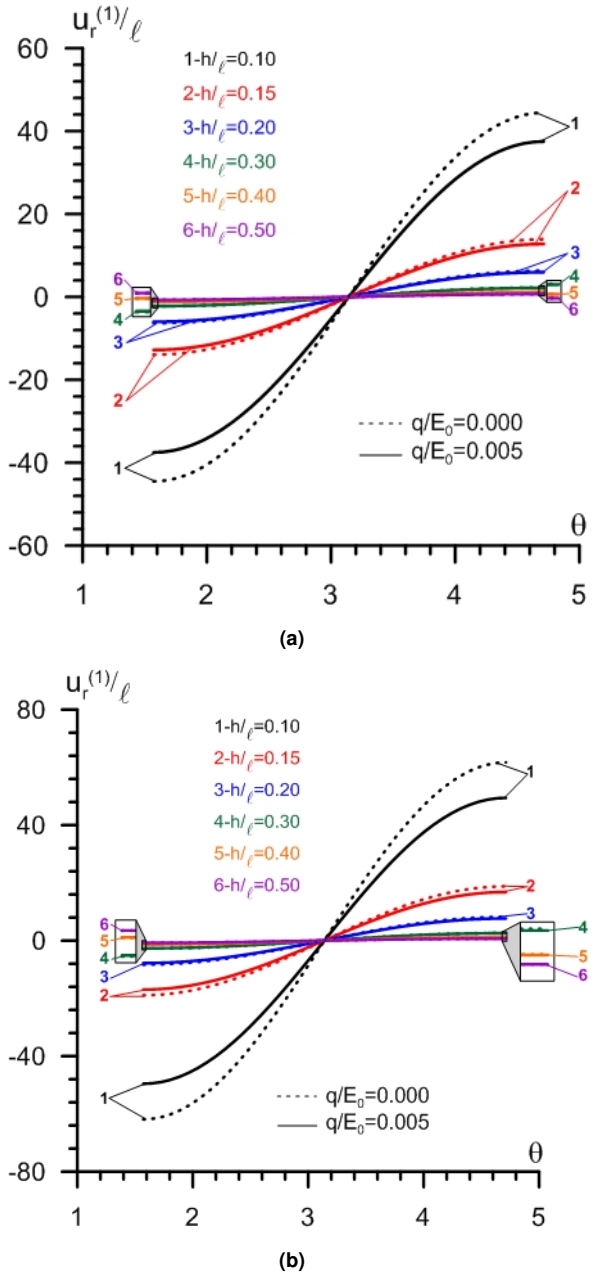

Fig. 10. The normalized radial displacement $u_r^{(1)}/\ell$ on the rim of circular hole around $\theta \in [-\pi/2, +\pi/2]$ for the different size of the plate-strip (i.e., h/ℓ) under $E_1/E_0 = 5$ $h_u/a = 5$ and $n = 2$ for two cases of q/E_O for (a) Problem 1 (b) Problem 2

crease of the power-law exponent value for $E_1/E_0 = 1$. The difference between the values obtained for n = 0.5 and n = 2 also decrease with E_1/E_0.

The angular position at which the normalized tangential and radial distributions become maximum is not affected either by the functional form of the material property gradation or the direction. The radial displacement is maximum at the poles $\theta = \pm\pi/2$ and reaches a minimum occurs at $\theta = \pi$, however the tangential displacement is maximum at the pole $\theta = \pi$ and reaches a minimum occurs at $\theta = \pm\pi/2$.

The effect of Young's Modulus ratio (E_1/E_0) on the nor-

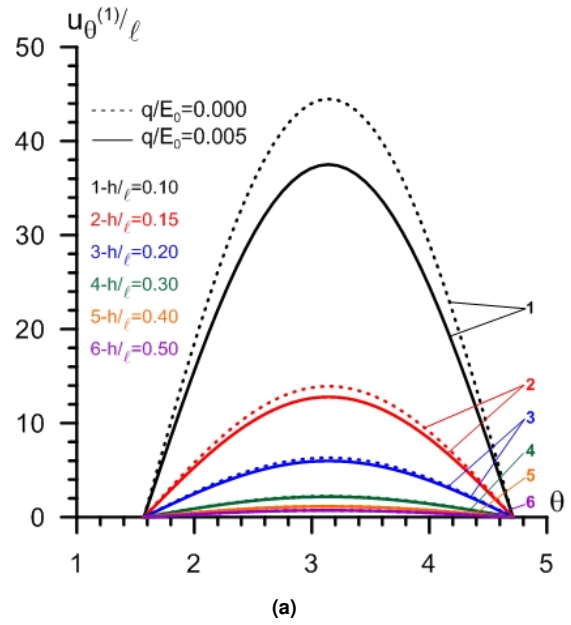

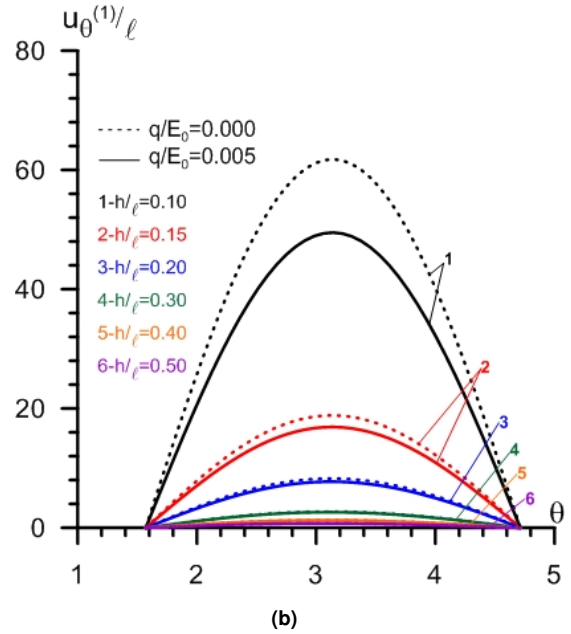

Fig. 11. The normalized tangential displacement $u_\theta^{(1)}/\ell$ on the rim of circular hole around $\theta \in [-\pi/2, +\pi/2]$ for the different size of the plate-strip (i.e., h/ℓ) under $E_1/E_0 = 5$, $h_u/a = 5$ and $n = 2$ for two case of q/E_0 for (a) Problem 1, (b) Problem 2.

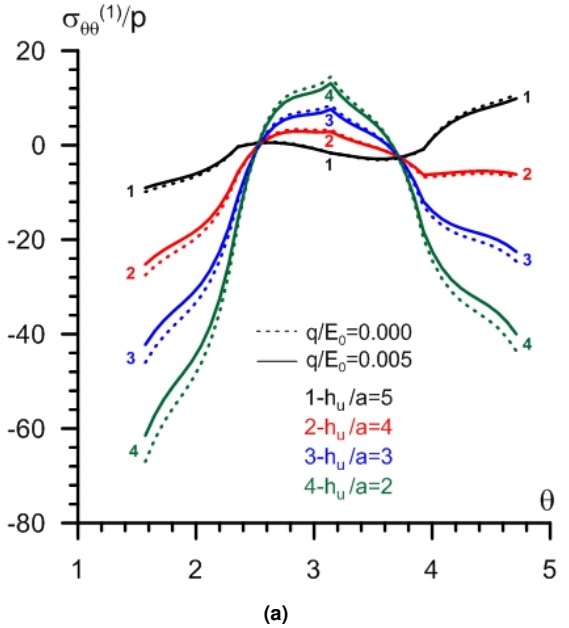

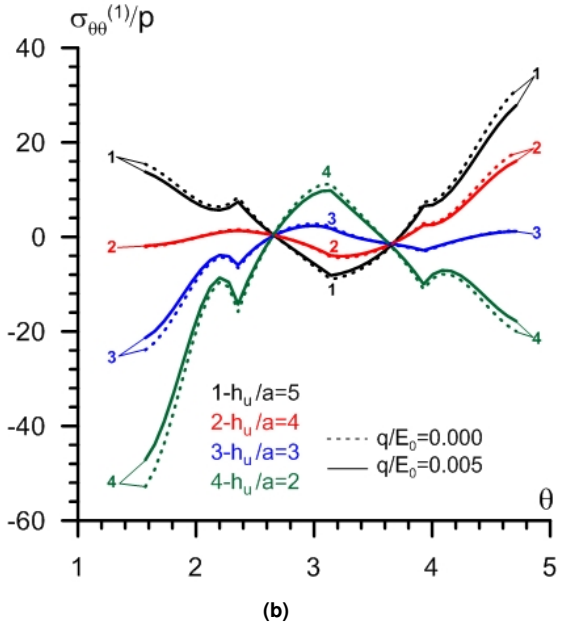

Fig. 12. The normalized tangential stress $\sigma_{\theta\theta}^{(1)}/p$ on the rim of circular hole around $\theta \in [-\pi/2, +\pi/2]$ for the different location of the hole (i.e., h_u/a) under $E_1/E_0 = 5$ $h/\ell = 0.15$ and $n = 2$ for two cases of q/E_0 for (a) Problem 1, (b) Problem 2

malized tangential stresses for some power-law exponents are presented for Problem 1 (Problem 2) in Table 2 (Table 3). The values of numerator of the fraction indicates the values of stress for $q/E_0 = 0$ (no initial stress), while the values of denominator of the fraction indicates the values of stress for $q/E_0 = 0.005$.

In Table 2, for Problem 1, it can be seen that for a certain power-law exponent (n), the normalized tangential stress increases absolutely with Young's Modulus ratio at the poles $\theta = \pm\pi/2, \pi$, while the stresses decrease absolutely at the pole $\theta = 3\pi/4$ and decrease at the pole $\theta = -3\pi/4$ with Young's Modulus ratio. Also, it can be seen that for a certain Young's Modulus ratio, the normalized tangential

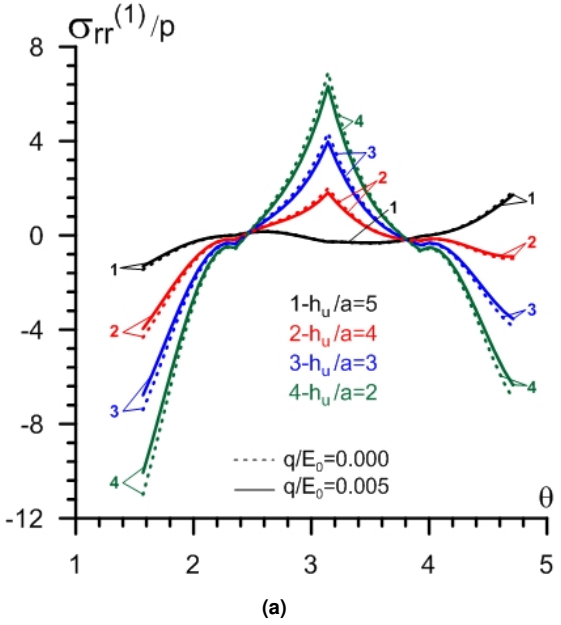

Fig. 13. The normalized radial stress $\sigma_{rr}^{(1)}/p$ on the rim of circular hole around $\theta \in [-\pi/2, +\pi/2]$ for the different location of the hole (i.e., h_u/a) under $E_1/E_0 = 5$ $h/\ell = 0.15$ and $n = 2$ for two cases of q/E_0 for (a) Problem 1 (b), Problem 2

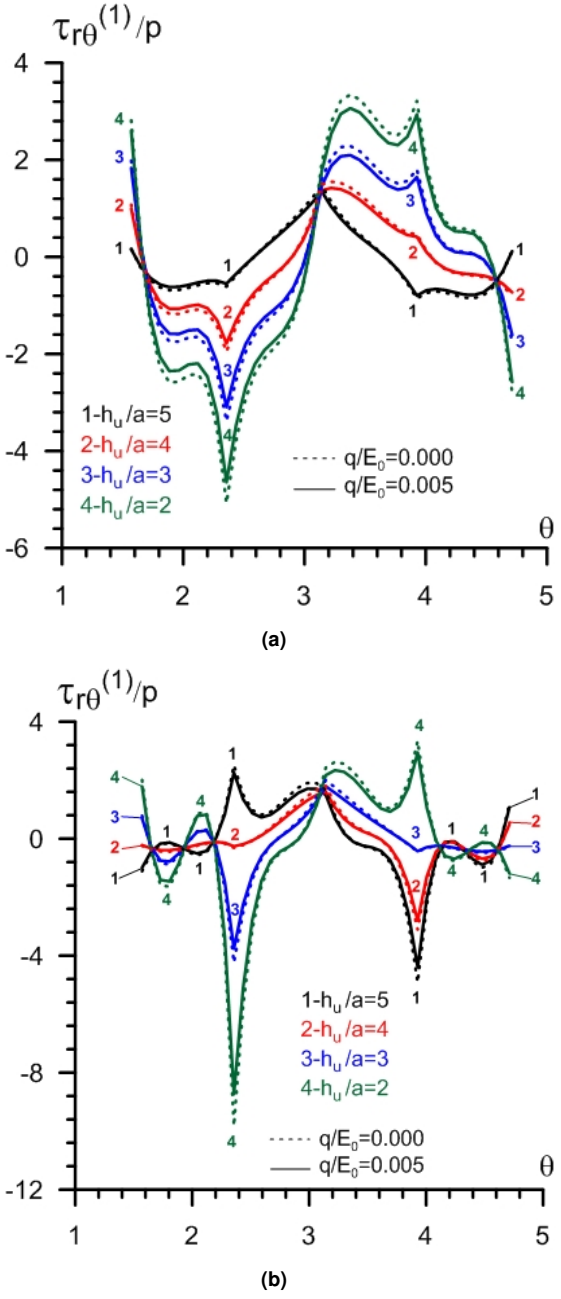

Fig. 14. The normalized shear stress $\tau_{r\theta}^{(1)}/p$ on the rim of circular hole around $\theta \in [-\pi/2, +\pi/2]$ for the different location of the hole (i.e., h_u/a) under $E_1/E_0 = 5$ $h/\ell = 0.15$ and $n = 2$ for two cases of q/E_0 for (a) Problem 1 (b), Problem 2.

stress increases absolutely with power- law exponent at the poles $\theta = \pm\pi/2, \pi$, while the stresses decrease absolutely at the pole $\theta = 3\pi/4$ and decrease at the pole $\theta = -3\pi/4$ with power-law exponent. The presence of initial stresses in the plate reduces the values of stresses and stresses are more affected by the variation of the Young's Modulus ratio and the power-law exponent for the case of the presence of the initial stresses.

In Table 3, for Problem 2, it can be seen that for a certain power-law exponent, the normalized tangential stress increases with Young's Modulus ratio at $\theta = \pm\pi/2, \pm 3\pi/4$ while the stresses decrease with Young's Modulus ratio

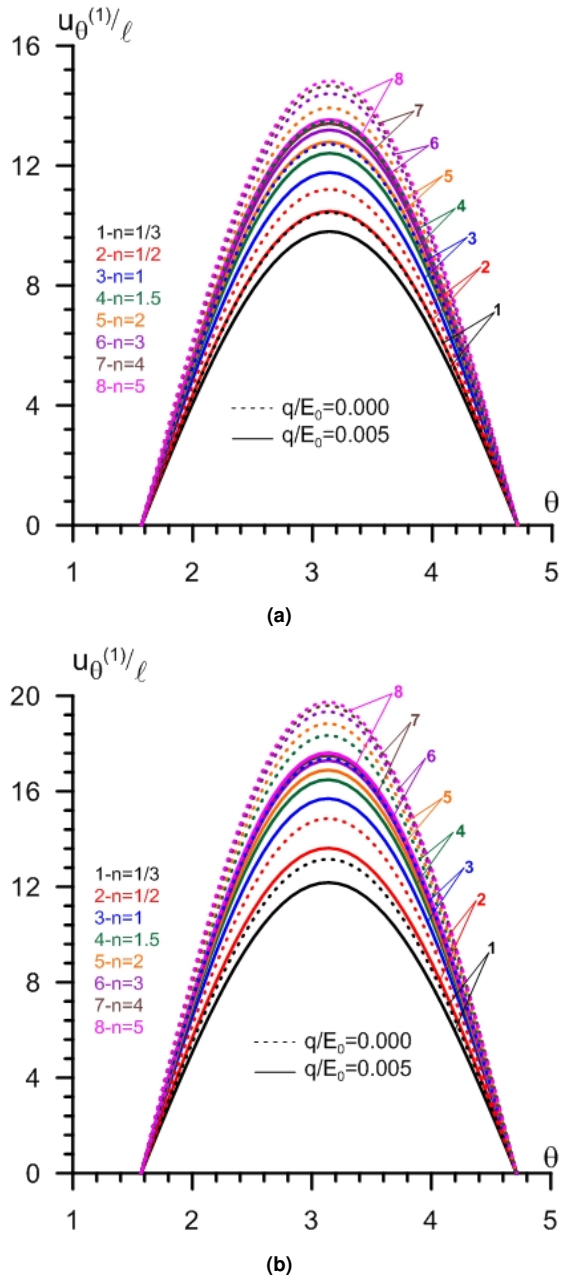

Fig. 15. The normalized tangential displacement $u_\theta^{(1)}/\ell$ on the rim of circular hole around $\theta \in [-\pi/2, +\pi/2]$ for the different power-law exponent (i.e. $\boldsymbol{n}$) under $E_1/E_0 = 5$ $h/\ell = 0.15$ and $h_u/a = 5$ for two cases of q/E_0 for (a) Problem 1 (b) Problem 2

at $\theta = \pi$. Also, it can be seen that for a certain Young's Modulus ratio, the normalized tangential stress increases absolutely with power-law exponent for $\mathbf{n} = 1/2 \rightarrow 2$, while, the stress decreases absolutely for $\mathrm{n} = 2 \rightarrow 5$, at $\theta = \pi/2, 3\pi/4$ for $(\mathrm{E}_1/\mathrm{E}_0 < 1)$, however the stresses increase absolutely with Young's Modulus ratio at $\theta = \pi/2, 3\pi/4$ for $(\mathrm{E}_1/\mathrm{E}_0 > 1)$. At $\theta = \pi$, the normalized tangential stress increases with power-law exponent for $n = 1/2 \rightarrow 2$, while, the stress decreases for $n = 2 \rightarrow 5$, for all values of Young's Modulus ratio. And at $\theta = -3\pi/2$ and $\pi/2$, the normalized tangential stress increases absolutely with power-law exponent for $(\mathrm{E}_1/\mathrm{E}_0 < 1)$, while the stresses increase for $\mathrm{n} = 1/2 \rightarrow 2$, but decrease for $\mathrm{n} = 2 \rightarrow 5$ with Young's Modulus ratio for $(\mathrm{E}_1/\mathrm{E}_0 > 1)$.

The results show that the normalized tangential stresses are affected more by the use of graded elements in Problem 2 than in Problem 1.

5. Conclusions

In this study, The Linearized Three-Dimensional Elasticity Theory is used to analyze the effect of pre-stresses on the plate-strip which include a circular hole under bending. The plate-strip's material is assumed functionally graded. Also the influence of grading direction on the static analysis of pre-stressed plate-strip is investigated. Using the FEM, influence of power-law exponent, location of hole, size of plate-strip and magnitude of prestresses on the displacements and the stresses on the rim of circular hole have been investigated. From the numerical results obtained, the following conclusions can be drawn:

- The initial compressive force affect the stresses and displacements much more than the initial stretching force,
- An increase in the absolute values of initial compressive force causes an increase in the absolute values of stresses and displacements,
- An increase in the absolute values of initial tension force causes a decrease in the absolute values of stresses and displacements,
- The variation of pre-stresses does not change the angular position of the maximum stresses and displacements, The absolute values of stresses and displacements decrease with plate size,
- The difference between the values of stresses and displacements obtained for $\mathrm{q}/\mathrm{E}_0 = 0$ and $\mathrm{q}/\mathrm{E}_0 = 0.005$ decrease with plate size,
- The absolute values of stresses increase with decreasing the distance between the upper face of the plate-strip and the upper surface of the circular hole,
- The displacements around the circular hole increase with the increase of the power-law exponent value, For a certain power-law exponent, the displacement

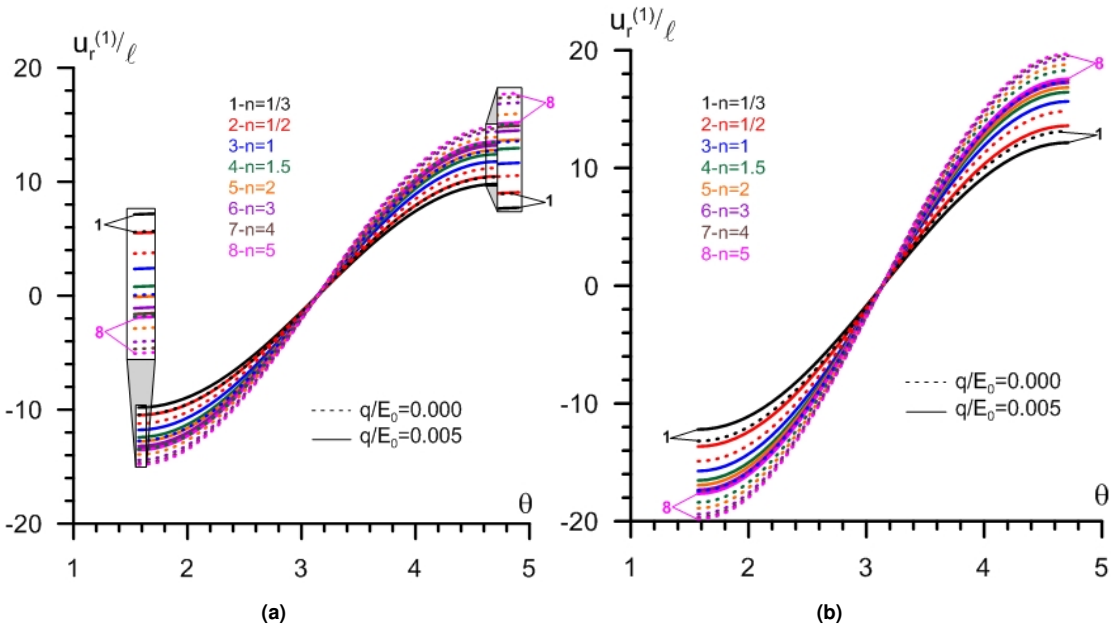

Fig. 16. The normalized radial displacement $u_r^{(1)}/\ell$ on the rim of circular hole around $\theta \in [-\pi/2, +\pi/2]$ for the different power-law exponent (i.e., $\boldsymbol{n}$) under $E_1/E_0 = 5$ $h/\ell = 0.15$ and $h_u/a = 5$ for two cases of q/E_O for (a) Problem 1, (b) Problem 2.

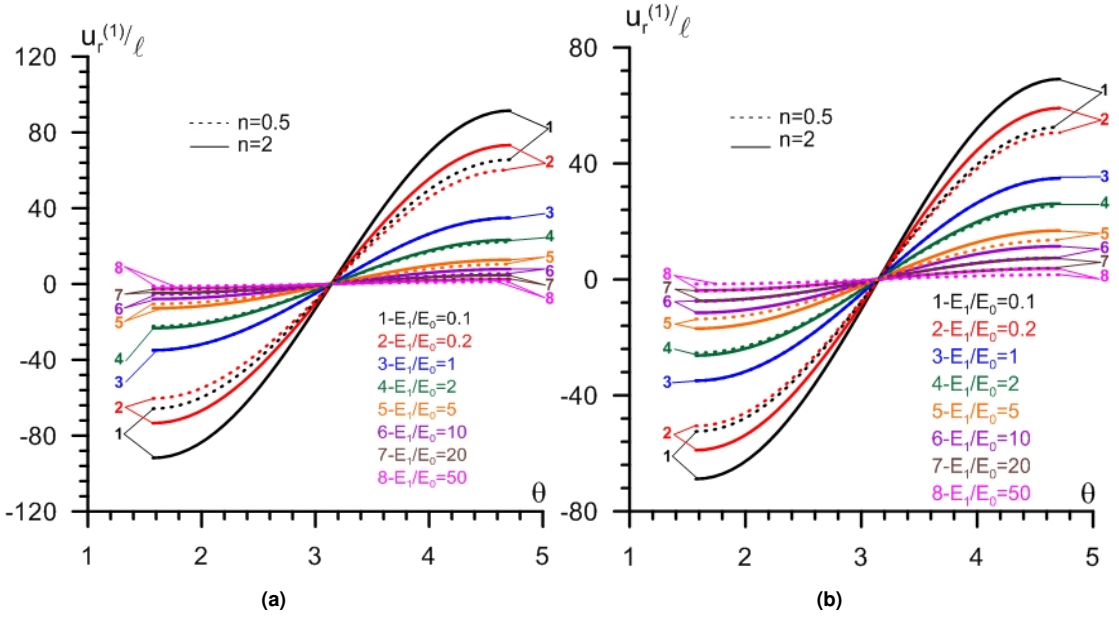

Fig. 17. The normalized radial displacement $u_r^{(1)}/\ell$ on the rim of circular hole around $\theta \in [-\pi/2, +\pi/2]$ for the different values of E_1/E_0, for two cases of $\mathbf{n}$ ($n = 0.5$ and $n = 2$) under $q/E_0 = 0.005$, $h/\ell = 0.15$, $h_u/a = 5$ for (a) Problem 1, (b) Problem 2.

decreases with Young's Modulus ratio, The amplitude of the displacements for the graded material for which the inhomogeneity is parallel to the direction of initial stresses and perpendicular to the bending force (Problem 1) is larger than the inhomogeneity is perpendicular to the direction of initial stresses and parallel to the bending force,

- The effects of the variation of the Young's Modulus

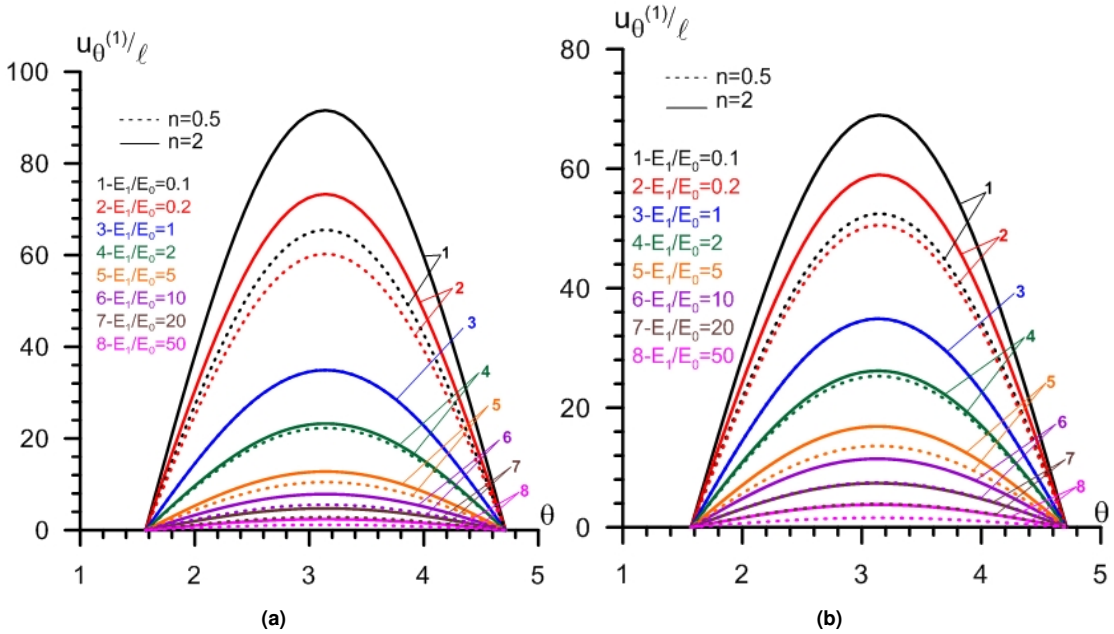

Fig. 18. The normalized tangential displacement $u_\theta^{(1)}/\ell$ on the rim of circular hole around $\theta \in [-\pi/2, +\pi/2]$ for the different values of E_1/E_0, for two cases of $n(n = 0.5$ and $n = 2$) under $q/E_0 = 0.005, h/\ell = 0.15, h_u/a = 5$ for (a) Problem 1, (b) Problem 2.

Table 2. Effect of Young's Modulus on $\sigma_{\theta\theta}^{(1)}/\ p$ at the poles $(\theta = \mp\pi/2, \pi, \mp 3\pi/4)$ around the circular hole for some power-law exponents for two cases of q/E_0 for Problem 1.

$\frac{\sigma_{\theta\theta}^{(1)}/\,\mathrm{p}\vert_{q/E_0=0}}{\sigma_{\theta\theta}^{(1)}/\,\mathrm{p}\vert_{q/E_0=0.005}}$	θ	E_1/E_0							
		0.1	0.2	1	2	5	10.0	20.0	50.0
n=1/2	$\frac{\pi}{2}$	$\frac{-7.6055}{-4.3071}$	$\frac{-8.9217}{-5.3575}$	$\frac{-9.7772}{-7.5231}$	$\frac{-9.8013}{-8.3599}$	$\frac{-9.8076}{-9.1286}$	$\frac{-9.8085}{-9.4500}$	$\frac{-9.8087}{-9.6247}$	$\frac{-9.8087}{-9.7341}$
	$\frac{3\pi}{4}$	$\frac{-2.1077}{-1.0662}$	$\frac{-1.2435}{-0.7822}$	$\frac{-0.3820}{-0.4211}$	$\frac{-0.3492}{-0.3872}$	$\frac{-0.3407}{-0.3611}$	$\frac{-0.3396}{-0.3506}$	$\frac{-0.3393}{-0.3450}$	$\frac{-0.3392}{-0.3415}$
	π	$\frac{-1.1314}{-1.0953}$	$\frac{-1.3131}{-1.2832}$	$\frac{-1.6106}{-1.6033}$	$\frac{-1.6257}{-1.6221}$	$\frac{-1.6294}{-1.6280}$	$\frac{-1.6299}{-1.6292}$	$\frac{-1.6300}{-1.6296}$	$\frac{-1.6300}{-1.6299}$
	$-\frac{3\pi}{4}$	$\frac{1.4386}{0.4513}$	$\frac{0.4235}{0.0070}$	$\frac{-0.6887}{-0.6376}$	$\frac{-0.7425}{-0.6984}$	$\frac{-0.7573}{-0.7345}$	$\frac{-0.7594}{-0.7471}$	$\frac{-0.7599}{-0.7536}$	$\frac{-0.7600}{-0.7575}$
	$-\frac{\pi}{2}$	$\frac{8.2652}{4.8975}$	$\frac{9.7741}{6.1439}$	$\frac{10.7118}{8.4380}$	$\frac{10.7180}{9.2660}$	$\frac{10.7172}{10.0342}$	$\frac{10.7169}{10.3565}$	$\frac{10.7169}{10.5319}$	$\frac{10.7169}{10.6418}$
n=2	$\frac{\pi}{2}$	$\frac{-9.4458}{-3.7103}$	$\frac{-9.5947}{-4.9374}$	$\frac{-9.7772}{-7.5231}$	$\frac{-9.8158}{-8.3097}$	$\frac{-9.8480}{-9.0171}$	$\frac{-9.8634}{-9.3514}$	$\frac{-9.8739}{-9.5646}$	$\frac{-9.8830}{-9.7268}$
	$\frac{3\pi}{4}$	$\frac{-0.8213}{-0.4274}$	$\frac{-0.6276}{-0.4719}$	$\frac{-0.3820}{-0.4211}$	$\frac{-0.3300}{-0.3754}$	$\frac{-0.2874}{-0.3223}$	$\frac{-0.2675}{-0.2923}$	$\frac{-0.2542}{-0.2707}$	$\frac{-0.2430}{-0.2521}$
	π	$\frac{-1.4182}{-1.3492}$	$\frac{-1.4998}{-1.4628}$	$\frac{-1.6106}{-1.6033}$	$\frac{-1.6346}{-1.6311}$	$\frac{-1.6537}{-1.6524}$	$\frac{-1.6623}{-1.6616}$	$\frac{-1.6677}{-1.6674}$	$\frac{-1.6721}{-1.6719}$
	$-\frac{3\pi}{4}$	$\frac{-0.0680}{-0.3663}$	$\frac{-0.3301}{-0.4309}$	$\frac{-0.6887}{-0.6376}$	$\frac{-0.7726}{-0.7211}$	$\frac{-0.8455}{-0.8081}$	$\frac{-0.8814}{-0.8554}$	$\frac{-0.9064}{-0.8893}$	$\frac{-0.9282}{-0.9189}$
	$-\frac{\pi}{2}$	$\frac{10.4161}{4.5282}$	$\frac{10.5704}{5.8257}$	$\frac{10.7118}{8.4380}$	$\frac{10.7251}{9.2091}$	$\frac{10.7267}{9.8918}$	$\frac{10.7230}{10.2090}$	$\frac{10.7183}{10.4080}$	$\frac{10.7126}{10.5559}$
n=5	$\frac{\pi}{2}$	$\frac{-9.5634}{-3.4602}$	$\frac{-9.6416}{-4.8099}$	$\frac{-9.7772}{-7.5231}$	$\frac{-9.8201}{-8.2987}$	$\frac{-9.8662}{-8.9856}$	$\frac{-9.8945}{-9.3161}$	$\frac{-9.9182}{-9.5370}$	$\frac{-9.9438}{-9.7208}$
	$\frac{3\pi}{4}$	$\frac{-0.6762}{-0.4025}$	$\frac{-0.5682}{-0.4541}$	$\frac{-0.3820}{-0.4211}$	$\frac{-0.3243}{-0.3717}$	$\frac{-0.2637}{-0.3046}$	$\frac{-0.2277}{-0.2601}$	$\frac{-0.1985}{-0.2229}$	$\frac{-0.1682}{-0.1845}$
	π	$\frac{-1.4762}{-1.4054}$	$\frac{-1.5249}{-1.4878}$	$\frac{-1.6106}{-1.6033}$	$\frac{-1.6372}{-1.6337}$	$\frac{-1.6647}{-1.6634}$	$\frac{-1.6805}{-1.6799}$	$\frac{-1.6929}{-1.6926}$	$\frac{-1.7049}{-1.7048}$
	$-\frac{3\pi}{4}$	$\frac{-0.2574}{-0.4326}$	$\frac{-0.4102}{-0.4689}$	$\frac{-0.6887}{-0.6376}$	$\frac{-0.7813}{-0.7279}$	$\frac{-0.8833}{-0.8402}$	$\frac{-0.9475}{-0.9140}$	$\frac{-1.0022}{-0.9773}$	$\frac{-1.0623}{-1.0459}$
	$-\frac{\pi}{2}$	$\frac{10.5496}{4.2865}$	$\frac{10.6201}{5.6995}$	$\frac{10.7118}{8.4380}$	$\frac{10.7292}{9.1965}$	$\frac{10.7343}{9.8497}$	$\frac{10.7309}{10.1505}$	$\frac{10.7225}{10.3403}$	$\frac{10.7064}{10.4830}$

Table 3. Effect of Young's Modulus on $\sigma_{\theta\theta}^{(1)}/\ p$ at the poles ($\theta = \mp\pi/2, \pi, \mp 3\pi/4$) around the circular hole for some power-law exponents for two cases of q/E_0 for Problem 2.

$\frac{\sigma_{\theta\theta}^{(1)}/\ \mathrm{p}\|_{\mathrm{q}/\mathrm{E}_0=0}}{\sigma_{\theta\theta}^{(1)}/\ \mathrm{p}\|_{\mathrm{q}/\mathrm{E}_0=0.005}}$	θ	E_1/E_0							
		0.1	0.2	1	2	5	10.0	20.0	50.0
n=1/2	$\frac{\pi}{2}$	$\frac{-39.1445}{-25.6426}$	$\frac{-35.2383}{-23.5418}$	$\frac{-9.7772}{-7.5231}$	$\frac{1.1659}{1.0163}$	$\frac{9.4515}{8.6470}$	$\frac{11.7338}{11.1805}$	$\frac{12.4660}{12.1594}$	$\frac{12.6975}{12.5700}$
	$\frac{3\pi}{4}$	$\frac{-7.0042}{-4.9999}$	$\frac{-6.2138}{-4.5207}$	$\frac{-0.3820}{-0.4211}$	$\frac{3.0236}{2.4677}$	$\frac{6.1846}{5.6151}$	$\frac{7.1449}{6.7853}$	$\frac{7.4615}{7.2662}$	$\frac{7.5627}{7.4820}$
	π	$\frac{5.8521}{3.2656}$	$\frac{4.8861}{2.7172}$	$\frac{-1.6106}{-1.6033}$	$\frac{-4.7351}{-4.2046}$	$\frac{-7.5083}{-6.9741}$	$\frac{-8.3512}{-8.0156}$	$\frac{-8.6289}{-8.4470}$	$\frac{-8.7175}{-8.6424}$
	$-\frac{3\pi}{4}$	$\frac{-11.1353}{-7.5871}$	$\frac{-9.7658}{-6.7931}$	$\frac{-0.6887}{-0.6376}$	$\frac{3.2063}{2.6328}$	$\frac{6.3309}{5.7575}$	$\frac{7.2341}{6.8756}$	$\frac{7.5269}{7.3330}$	$\frac{7.6197}{7.5396}$
	$-\frac{\pi}{2}$	$\frac{-13.3695}{-8.5353}$	$\frac{-10.3517}{-6.6979}$	$\frac{10.7118}{8.4380}$	$\frac{20.6986}{17.4130}$	$\frac{28.8777}{26.3851}$	$\frac{31.2854}{29.7941}$	$\frac{32.0882}{31.2909}$	$\frac{32.3482}{32.0200}$
n=2	$\frac{\pi}{2}$	$\frac{-55.6655}{-30.3309}$	$\frac{-41.4503}{-25.3962}$	$\frac{-9.7772}{-7.5231}$	$\frac{1.9816}{1.6873}$	$\frac{15.3965}{13.7519}$	$\frac{23.8236}{22.0839}$	$\frac{30.6796}{29.2328}$	$\frac{37.3917}{36.4829}$
	$\frac{3\pi}{4}$	$\frac{-9.2368}{-5.9533}$	$\frac{-7.1800}{-4.9591}$	$\frac{-0.3820}{-0.4211}$	$\frac{3.2185}{2.6117}$	$\frac{8.3916}{7.4512}$	$\frac{12.3932}{11.4601}$	$\frac{16.1929}{15.4104}$	$\frac{20.5111}{20.0019}$
	π	$\frac{10.5873}{4.9362}$	$\frac{6.7699}{3.4684}$	$\frac{-1.6106}{-1.6033}$	$\frac{-4.8501}{-4.2806}$	$\frac{-8.9645}{-8.1362}$	$\frac{-11.9941}{-11.2005}$	$\frac{-14.8569}{-14.2056}$	$\frac{-18.1316}{-17.7144}$
	$\frac{3\pi}{4}$	$\frac{-20.8360}{-11.9120}$	$\frac{-13.7179}{-8.7856}$	$\frac{-0.6887}{-0.6376}$	$\frac{3.2631}{2.6603}$	$\frac{7.3706}{6.5536}$	$\frac{9.8148}{9.0854}$	$\frac{11.7525}{11.1933}$	$\frac{13.5995}{13.2678}$
	$-\frac{\pi}{2}$	$\frac{-34.9843}{-18.8343}$	$\frac{-19.6794}{-11.8330}$	$\frac{10.7118}{8.4380}$	$\frac{20.7049}{17.2982}$	$\frac{31.1970}{27.8379}$	$\frac{37.1885}{34.4471}$	$\frac{41.6008}{39.6146}$	$\frac{45.3589}{44.2391}$
n=5	$\frac{\pi}{2}$	$\frac{-55.0559}{-28.5379}$	$\frac{-41.0178}{-24.6642}$	$\frac{-9.7772}{-7.5231}$	$\frac{2.0538}{1.7446}$	$\frac{15.7377}{13.9828}$	$\frac{24.5253}{22.5518}$	$\frac{31.9333}{30.1342}$	$\frac{39.6330}{38.3081}$
	$\frac{3\pi}{4}$	$\frac{-9.0466}{-5.7289}$	$\frac{-7.1050}{-4.8625}$	$\frac{-0.3820}{-0.4211}$	$\frac{3.2260}{2.6140}$	$\frac{8.4655}{7.4767}$	$\frac{12.6682}{11.6186}$	$\frac{16.9402}{15.9634}$	$\frac{22.4267}{21.6611}$
	π	$\frac{10.5242}{4.5525}$	$\frac{6.7107}{33.283}$	$\frac{-1.6106}{-1.6033}$	$\frac{-4.8430}{-4.2710}$	$\frac{-8.8741}{-8.0203}$	$\frac{-11.7866}{-10.9287}$	$\frac{-14.5537}{-13.7916}$	$\frac{-17.8236}{-17.2580}$
	$-\frac{3\pi}{4}$	$\frac{-21.8256}{-11.9376}$	$\frac{-13.9717}{-8.8028}$	$\frac{-0.6887}{-0.6376}$	$\frac{3.2430}{2.6395}$	$\frac{7.2238}{6.3886}$	$\frac{9.4805}{8.7056}$	$\frac{11.1702}{10.5373}$	$\frac{12.6108}{12.1898}$
	$-\frac{\pi}{2}$	$\frac{-37.0866}{-18.9981}$	$\frac{-20.3941}{-12.0399}$	$\frac{10.7118}{8.4380}$	$\frac{20.6215}{17.2055}$	$\frac{30.7641}{27.3072}$	$\frac{36.3613}{33.4052}$	$\frac{40.2880}{37.9849}$	$\frac{43.1439}{41.6715}$

ratio and the power-law exponent are more in the case where the presence of the initial stresses.

- The normalized tangential stresses are affected more by the use of graded elements in Problem 2 than in Problem 1.

Acknowledgement

The authors are grateful to Prof. Dr. Nazmiye Yahnioglu for comments, discussions and considerable revision of the manuscript.

References

[1] M Koiwumi. The concept of FGM, Ceram. Trans. Func. Grad. Mater., 34, 3-10. In *Linear Networks and Systems*, pages 123–135. Berlmont, CA, 1993.

[2] F Erdogan and B. H. Wu. The surface crack problem for a plate with functionally graded properties. *Journal of Applied Mechanics, Transactions ASME*, 64(3):449–456, 1997.

[3] J N Reddy, C M Wang, and S Kitipornchai. Axisymmetric bending of functionally graded circular and annular plates. *European Journal of Mechanics-A/Solids*, 18(2):185–199, 1999.

[4] M H Santare and J Lambros. Use of graded finite elements to model the behavior of nonhomogeneous materials. *Journal of Applied Mechanics, Transactions ASME*, 67(4):819–822, 2000.

[5] Jeong Ho Kim and G H Paulino. Isoparametric graded finite elements for nonhomogeneous isotropic and orthotropic materials. *Journal of Applied Mechanics, Transactions ASME*, 69(4):502–514, 2002.

[6] Shyang Ho Chi and Yen Ling Chung. Mechanical behavior of functionally graded material plates under transverse load-Part I: Analysis. *International Journal of Solids and Structures*, 43(13):3657–3674, 2006.

[7] Shyang Ho Chi and Yen Ling Chung. Mechanical behavior of functionally graded material plates under transverse load-Part I: Analysis. *International Journal of Solids and Structures*, 43(13):3657–3674, 2006.

[8] D. V. Kubair and B. Bhanu-Chandar. Stress concentration factor due to a circular hole in functionally graded panels under uniaxial tension. *International Journal of Mechanical Sciences*, 50(4):732–742, 2008.

[9] B Yang, H.J Ding, and W.Q Chen. Elasticity solutions

for a uniformly loaded annular plate of functionally graded materials. *Structural Engineering and Mechanics*, 30(4):501–512, 2008.

[10] Quanquan Yang, Cun Fa Gao, and Wentao Chen. Stress analysis of a functional graded material plate with a circular hole. *Archive of Applied Mechanics*, 80(8):895–907, aug 2010.

[11] Quan Quan Yang, Cun Fa Gao, and Wen Tao Chen. Stress concentration in a finite functionally graded material plate. In *Science China: Physics, Mechanics and Astronomy*, volume 55, pages 1263–1271, jul 2012.

[12] Gururaja Udupa, S. Shrikantha Rao, and K.V. Gangadharan. Functionally Graded Composite Materials: An Overview. *Procedia Materials Science*, 5:1291–1299, 2014.

[13] Dinh Kien Nguyen, Buntara S. Gan, and Thanh Huong Trinh. Geometrically nonlinear analysis of planar beam and frame structures made of functionally graded material. *Structural Engineering and Mechanics*, 49(6):727–743, 2014.

[14] A Chegenizadeh, B Ghamidi, H Nikraz, and M Simsek. A novel two-dimensional approach to modelling functionally graded resting on a soil medium. *Structural Engineering and Mechanisms*, 51(5):727–741, 2014.

[15] Tran Minh Tu, Tran Huu Quoc, and Nguyen Van Long. Bending analysis of functionally graded plates using new eight-unknown higher order shear deformation theory. In *Structural Engineering and Mechanics*, volume 62, pages 311–324, 2017.

[16] Emrah Madenci. A refined functional and mixed formulation to static analyses of fgm beams. *Structural Engineering and Mechanics*, 69(4):427–437, 2019.

[17] Mourad Khebizi, Hamza Guenfoud, Mohamed Guenfoud, and Rached El Fatmi. Three-dimensional modelling of functionally graded beams using Saint-Venant's beam theory. *Structural Engineering and Mechanics*, 72(2):257–273, 2019.

[18] Pınar Aydan Demirhan and Vedat Taşkin. Static analysis of simply supported functionally graded sandwich plates by using four variable plate theory. *Teknik Dergi/Technical Journal of Turkish Chamber of Civil Engineers*, 30(2):8987–9007, 2019.

[19] S.D. Akbarov and A.N. Guz. *Mechanics of curved composites*. Kluwer Academic Publishers, Dordrecht, The Netherlands, 2000.

[20] O.C Zienkiewicz and R.L Taylor. *The Finite Element Methods: basic Formulation Linear Problems*. Oxford, mc graw-hi edition, 1989.

[21] G.N Savin. *Stress Concentration Around Holes*. Oxford, pergamon edition, 1951.

[22] S D Akbarov, N Yahnioglu, and U Babuscu Yesil. Interaction between two neighboring circular holes in a prestretched simply supported orthotropic strip under bending. *Mechanics of Composite Materials*, 44(6):581–590, 2008.

[23] S.P Timoshenko and J.N Goodier. *Theory of Elasticity*. London, third edit edition, 1970.